

COMPETING FEEDBACK IN AN IDEALIZED TIDE-INFLUENCED DELTA NETWORK

NON-PEER REVIEWED MANUSCRIPT SUBMITTED FOR CONSIDERATION IN *Environmental Fluid Mechanics*
DECEMBER 1, 2021

Niccolò Ragno^{1*}, Nicoletta Tambroni¹, and Michele Bolla Pittaluga¹

¹Department of Civil, Chemical and Environmental Engineering, University of Genoa, Via Montallegro 1, 16145 Genoa, Italy

ABSTRACT

The morphodynamic evolution of river deltas is intimately tied to flow and sediment partitioning at bifurcations. In this work, we investigate the long-term equilibrium configuration of a simple delta network using an analytical model, which accounts for the effect of small tidal oscillations. Differently from individual bifurcations, where tidal action is always a stabilizing factor, in the case of a tree-like delta with multiple bifurcations a dual response emerges. Specifically, depending on the values of four reference parameters function of tidal amplitude, upstream flow conditions, and on the geometry of the channels, tides can either promote or discourage an unbalanced discharge distribution. This behavior primarily concerns the apex bifurcation, which is affected by the variations of the relative tidal amplitude at the internal nodes. In turn these variations depend on how flow and sediment are diverted upstream. Finally, we discuss the outcomes of the model performing a qualitative comparison with field and experimental tide-influenced deltas. Results highlight the need of including in a unified scheme river-influenced (i.e. depositional) and tide-influenced (i.e. erosional) effects.

Keywords Bifurcations · Tide-influenced deltas · Steady states · Feedback mechanisms

1 INTRODUCTION

We are concerned with the morphodynamics of channel bifurcations, a representative geomorphological feature controlling the downstream flow routing in a variety of environmental settings such as coastal plains, mountain valleys, coastal wetlands, submarine fans, and lava flows [1, 2, 3, 4, 5, 6]. Here, we restrict our attention on river deltas, depositional landforms arising from rivers that end at the shoreline often originating a network of channels (Fig. 1).

A large number of studies performed to date provided a fairly clear picture of stability conditions for individual river bifurcations [7, 8], where the word “stability” is used throughout the paper in its mathematical sense, thus referring to the, either symmetrical or asymmetrical, state the bifurcation may take depending on the values of the relevant control parameters. However, in multi-thread rivers as deltas, bifurcations are not isolated elements but rather part of an interactive system [9, 10, 11]. Taking the viewpoint of complex networks [12, 13], competing interactions break-up the possibility of understanding the whole behavior of the system just by a superimposition of the single bifurcation responses. The latter statement raises a related question: what are the physical processes responsible for such interactions? The flux partitioning in the upstream bifurcations affects each subsequent downstream bifurcation by changing flow and sediment transport conditions in the connecting channels. However, this upstream-to-downstream “signal propagation” is not sufficient to generate a connection: a downstream-to-upstream influence is necessary as well.

In a series of recent works, Salter et al. [14, 15, 16] have shown that a net-depositional system is able to generate a switching in the discharge partitioning over time. The oscillations are purely autogenic, inasmuch they derive from an internal feedback mechanism: if the fluxes are distributed unevenly by a bifurcation, the slope of the channel receiving more sediment becomes lower through time with respect to the other channel, till eventually causing the switching [17]. Interestingly, a (deterministic) chaotic dynamics is observed when multiple bifurcations are coupled in a simple delta network [16].

A similar behavior, in which feedback mechanisms are internally generated, has been observed in a bifurcation-confluence system (i.e. a loop), where a river splits into two smaller anabranches rejoining downstream [18]. In this case, the feedback manifests in the differential water surface elevation in the downstream branches depending on the amount of water and sediment delivered by the bifurcation, which results in an asymmetric energy slope affecting discharge partition upstream.

In this paper, we aim at understanding how tides potentially affect the long-term equilibrium state of river deltas and, in particular, how the system adjusts to varying geometric and flow conditions. To achieve this goal, we pursue the one-dimensional modeling of an idealized delta network made up of multiple bifurcations, with branching channels flowing into a tidal sea. Tidal influence is considered small enough so that the morphodynamics of the delta is primarily controlled by fluvial processes. We explicitly excluded wave activity that, basically through an alongshore sediment transport [19], is responsible for several morphological implications including the suppression of bifurcations near the coastline [20, 21].

*correspondence: niccolo.ragno@edu.unige.it



Figure 1: Example: the Northern Dvina Delta, near the city of Arkhangelsk (Russia), $64^{\circ}32' \text{ N } 40^{\circ}32' \text{ E}$. Image credit: Google Earth Pro (2021).

The analysis is motivated by recent theoretical advances on individual tide-influenced bifurcations [22], showing that tidal action causes a morphodynamic response akin to the one observed by Salter et al. [14], but due to an opposite underlying physical process: tide deepens downstream channels through erosion, leading the branch carrying the smaller amount of water and sediment to increase its slope over time with respect to the other branch. However, this behavior might not be univocal when bifurcations are combined in series in a tree-like structure, inasmuch the response of upstream bifurcations depends from the water surface elevation at the internal nodes downstream, which is different from the tidal amplitude seaward.

The rest of the paper proceeds as follows. The main achieved results on the stability of individual bifurcations in fluvial environments and under tidal influence are briefly reviewed in Sections 2.1 and 2.2. Section 3 introduces the theoretical framework for the long-term equilibrium of a tide-influenced delta composed by a generic number of bifurcations, while in Section 4 the outcomes of the model are restricted to a small network consisting of two orders of branches. We discuss the implications and possible future developments of the model in Section 5.

2 BACKGROUND

2.1 Stability of individual bifurcations in fluvial environments

Over the last three decades, river bifurcations in fluvial environments have been investigated through a breadth of different approaches, including theoretical [23, 24, 7, 25], experimental [26, 27, 28], numerical [29, 30, 31, 32], and field studies [33, 34, 35, 36]. Morphodynamic modeling involved mainly one-dimensional schemes able to represent in a simplified way the complex flow-routing processes that characterize real world bifurcations. Notably, in these models the partition of water and sediment fluxes in the downstream branches requires the adoption of a suitable nodal relationship. In this paper, we follow the widely-employed two-cell model originally proposed by Bolla Pittaluga et al. [37] (hereafter, BRT). We refer to [8, 17] for a synthesis of the model, and we limit ourselves to recall the key outcomes.

In the ideal absence of external “forcing” factors induced by the surrounding environment, the morphodynamic evolution of a perfectly symmetrical (i.e. “free”, sec. [25]) bifurcation is governed by a unique parameter, \mathcal{R} [26, 7]:

$$\mathcal{R} = \frac{r\alpha}{\beta_0 \sqrt{\tau_{*0}}}, \quad (1)$$

where τ_{*0} (hereafter, the suffix $_0$ refers to the main upstream channel) is the Shields number of the feeder channel, and β_0 is the width-to-depth ratio. The parameter α is an order-one parameter physically representing the (dimensionless) extension of a

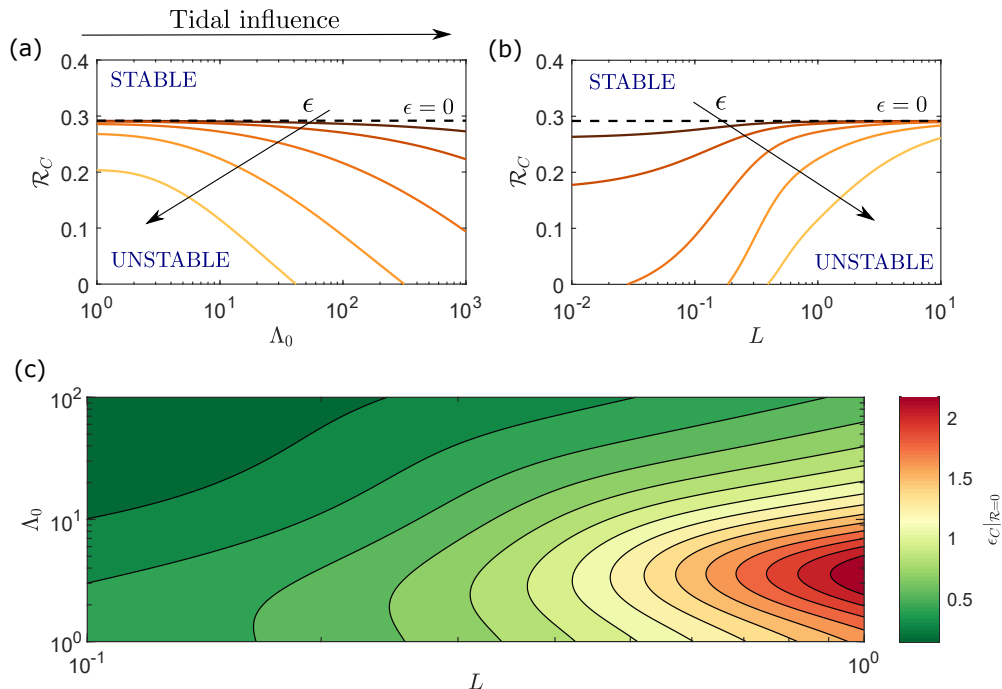


Figure 2: Example solution obtained from the stability analysis performed by RTB [22]. The critical threshold of \mathcal{R} is reported for increasing values of the scaled tidal amplitude ϵ , which spans within $\epsilon = 0$ (i.e. absence of tide, black dashed line) and $\epsilon = 0.8$, as a function of (a) Λ_0 ($L = 1$) and (b) L ($\Lambda_0 = 10$). The value of \mathcal{R} separating the stable/unstable solution decreases as long as the tides is increased for sufficiently high/low values of Λ_0/L . In panel (c), it is reported the tidal threshold in the limiting case $\mathcal{R} = 0$.

transverse bed elevation gradient induced in the feeder channel by the bifurcation [25]. The sediment flux is deflected with respect to the water flow direction due to a gravitational effect, whose magnitude is controlled by the parameter r [38, 39].

The ‘‘bifurcation’’ parameter \mathcal{R} controls the number of equilibrium solutions and the stability of those equilibria: if \mathcal{R} is higher than a critical threshold \mathcal{R}_C , which depends on the friction and the transport formula adopted [8], the bifurcation keeps stable and equally distributes water and sediment fluxes; on the contrary, when \mathcal{R} is lower than the critical threshold, the balanced solution becomes unstable and the system attains a stable state where one of the two branches captures most of discharge, where at the same time, the gravitational pull deviates the sediment flux to prevent the closure of the penalized branch (i.e. carrying the lowest discharge). Notably, \mathcal{R} assumes the role of a bifurcation parameter also in a mathematical sense. Indeed, the equilibrium diagram is represented by a supercritical pitchfork bifurcation [40], where one/two possible steady states are possible whether \mathcal{R} is higher/lower than the threshold.

2.2 The stabilizing effect of tides in a single bifurcation

In low relief systems such as deltas, bifurcations are affected by different factors that change the picture depicted in the previous Section. In particular, downstream effects like a differential sedimentation [14, 15] or marine processes like tides [41, 42, 43, 44, 22], influence the response of bifurcations through variations of the channel slope, thereby introducing a dependence on the downstream channel lengths [18]. It is worth recalling that the BRT model does not produce any (internal) slope asymmetry at equilibrium, which is equivalent to infinite channel lengths.

In this paper, we focus our attention on the role of tides starting from the work of Ragno et al. [22] (hereafter, RTB), which included in the BRT model the effect of (monochromatic) tidal oscillations. Under the assumption of tidal amplitudes a^* (from hereinafter the superscript $*$ denotes a dimensional quantity) much smaller than the mean flow depth in the upstream channel D_0^* , RTB investigated stability conditions building on the previous work of Seminara et al. [45] for the (tidally-averaged) equilibrium of a single river-dominated estuary. When tides are taken into account, three other parameters turn out to play a role, namely the scaled tidal amplitude ϵ , a parameter measuring the relative importance of flow inertia Λ_0 , and the (dimensionless) average length of the branches L :

$$\epsilon := \frac{a^*}{D_0^*}, \quad \Lambda_0 := \frac{\omega^* L_{B0}^*}{U_0^*}, \quad L := \frac{L^*}{L_{B0}^*}, \quad (2)$$

where ω^* is the frequency of the tidal wave, U_0^* is the flow velocity of the feeder channel, and L_{B0}^* is the so-called backwater length [46], defined as the ratio between the flow depth D_0^* and the channel slope S_0 . The parameter Λ_0 is a representative indicator of the

tidal influence, as suggested by the proportionality to the backwater length; in alternative, assuming the reference Froude number $F_0 \approx \epsilon$, as typically encountered in natural low-lying rivers, the parameter Λ_0 can be rewritten as follows:

$$\Lambda_0 = \frac{\omega^* L_{B0}^*}{F_0 \sqrt{g^* D_0^*}} \approx \frac{L_{B0}^*}{T^* \epsilon \sqrt{g^* D_0^*}}, \quad F_0 = \frac{U_0^*}{\sqrt{g^* D_0^*}} \ll 1, \quad (3)$$

where g^* is the gravity acceleration, and $T^* = 2\pi/\omega^*$ the tidal period. Essentially, Λ_0 is the ratio between the time required for a tidal wave to travel for a reach as long as the backwater length, and the tidal period.

The (linear) stability analysis performed by RTB shows that tide acts as a negative feedback, since it promotes the stability of the bifurcation. For a given value of ϵ , the magnitude of this stabilizing effect increases as the branches are shortened and/or Λ_0 is amplified (Fig. 2a-b). Interestingly, if the tidal influence is sufficiently strong there is the possibility for a balanced configuration in which discharge is equally divided even in the limiting case where the gravitational effect at the bifurcation is negligible (i.e. $\mathcal{R} \rightarrow 0$) (Fig. 2c). In other words, the theoretical model suggests that for a given value of the parameters Λ_0 and L , there exists a ‘‘tidal threshold’’ that allows for a stable (balanced) bifurcation even in rivers where the sediment transport is purely suspended-dominated. In such conditions, the stability of the bifurcation is purely downstream-controlled by tidal action.

However, why this happens physically? When \mathcal{R} is small (i.e. the main channel is particularly wide and shallow), a greater fraction of water and sediment fluxes is steered towards one of the two branches. In this case, the tidal action tends to re-equilibrate the bifurcation by increasing the (bed) slope of the penalized branch, and thus generating a negative gradient, leading to an increased stability of the system.

2.3 Observed values of the relevant parameters in field and experimental deltas

A spontaneous question is what values do the relevant dimensionless parameters controlling the stability of tide-influenced bifurcations typically attain in real deltas. Estimated values of $(\mathcal{R}, \Lambda_0, L)$ for several natural and experimental deltas are reported in Fig. 3, as a function of the scaled tidal amplitude ϵ . Specifically, the analysis is based on two sets of laboratory experiments, performed by Lentsch et al. [47], and sixteen natural rivers forming deltaic distributary networks, which are characterized by different climatic settings (e.g., the Arctic Yukon, the Mediterranean Nile), morphology (e.g., lobe size and shape, number of distributary channels), and marine processes (i.e. waves and tides). We note that deltas are selected with the only purpose of understanding the typical range of magnitude of the different parameters. In this respect, we do not rely on the classic triad of river-, wave-, or tide-dominance [48, 20, 49]. Nevertheless, we avoid to consider deltas where the value of the scaled tidal amplitude (ϵ) is of the order of $O(1)$ or higher, as they exceed the limit of validity of the RTB model.

Values of the parameter Λ_0 spans within the range $10^0 - 10^2$, whereas \mathcal{R} ranges between 10^{-1} and 10^{-3} . As the majority of deltas analyzed in Fig. 3 are constituted by gentle-slope fine-grained rivers characterized by high-mobility conditions (i.e. high values of the Shields number), the low values of \mathcal{R} are not surprising (see Eq. 1). According to the sole bifurcation model, this would imply that almost all the bifurcations in the analyzed deltas should be invariably unstable, and thus strongly unbalanced. Consequently, the uneven distribution of flow and sediment transport should reflect in a strong asymmetry of the channel width in the distributaries of the networks. Nonetheless, this is not the case, for example, in the Mahakam Delta, where a number of field and numerical studies indicate how bifurcations in the network are characterized by a more uniform discharge distribution than the one that would occur in a purely riverine environment [55, 56]. Finally, as a reference length scale of the maximum distance where the apex node is placed, we investigate the order of magnitude of the so-called ‘‘avulsion length’’ ($L_A := L_A^*/L_{B0}^*$). The avulsion length, defined as the distance from the coastline of the apex node [20, 57], varies between 10^{-1} and 10^0 (Fig. 3c), suggesting that even micro-tidal conditions are sufficient to actively affect the apex node (see Fig. 2a-b).

3 A SIMPLE MODEL FOR THE EQUILIBRIUM OF TIDE-INFLUENCED DELTA NETWORKS

In Section 2.2, we have seen that in the case of a single bifurcation tides exert a stabilizing effect that prevents the closure of one of the two branches in the long-term. However, deltaic networks are formed by several interconnected bifurcations that can interact with each other [58, 59, 60, 61, 16].

Let us consider an ideal delta network, which is assumed to be composed by k orders of bifurcations. As a consequence, the number of nodes (N) of the system is equal to:

$$N = \sum_{j=1}^k 2^{j-1}. \quad (4)$$

Following RTB, each branch of the network is a straight estuary, where the banks are fixed (i.e. the planform geometry does not change in time), and the bottom is composed by a uniform sand with a reference grain size d^* . Seaward, debouching channels are subject to monochromatic tidal oscillations with a constant amplitude in the assumption $\epsilon \ll 1$. Landward, the main upstream channel is fed by a constant discharge Q_0^* , with the flow carrying a constant sediment flux in equilibrium with fluid flux Q_{s0}^* .

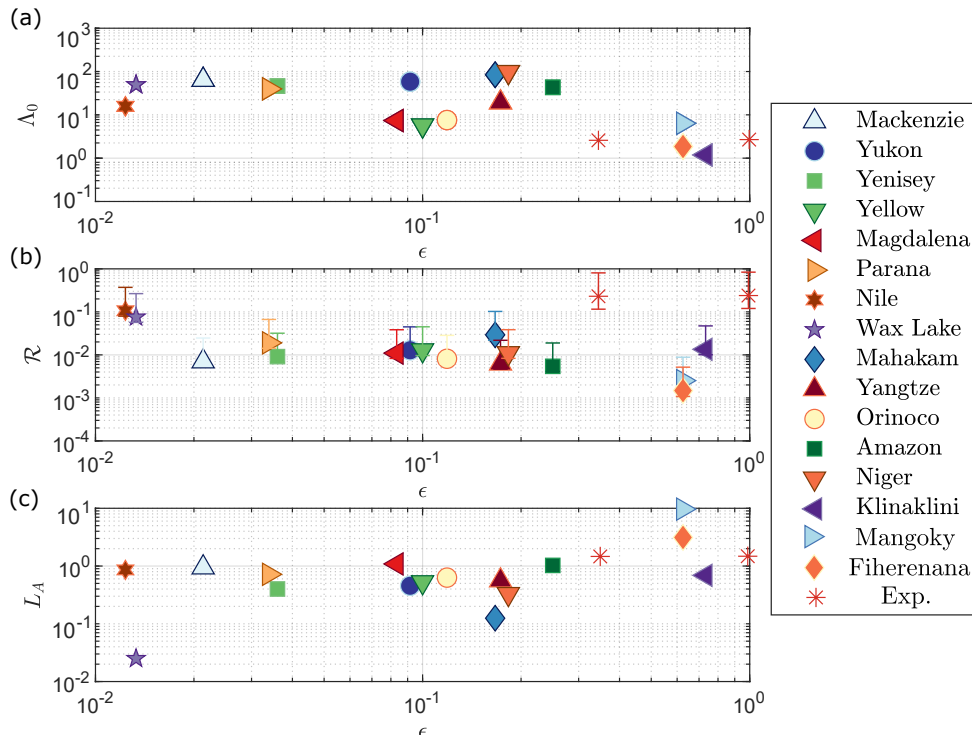


Figure 3: Relevant dimensionless parameters controlling the stability of tide-influenced bifurcations for a series of natural and experimental deltas. Panel (a) Λ_0 , (b) \mathcal{R} , and (c) L_A are shown as a function of the scaled tidal amplitude ϵ . The whisker in panel (b) represent the value of \mathcal{R} for $r\alpha = 0.5$ and $r\alpha = 5$. Sources: [50, 51, 42, 47, 52, 53, 54].

The geometry of the network (i.e. lengths ℓ^* and widths W^*) is assumed to be symmetric with respect to each node. Channel widths are assigned following hydraulic geometry laws empirically derived from delta networks. Specifically, we rely on the relationships derived by Andr n [62], which have been employed and tested against field and modeling studies [63, 64]:

$$W^* \propto Q^{*0.39} \rightarrow W^* \simeq \left(\frac{3}{4}\right)^k W_0^*, \quad (5)$$

where W_0^* is the width of the upstream feeder channel.

Analogously, each subsequent bifurcation is placed at a distance that follows a power-law distribution [63, 65, 64]:

$$\ell^* \propto Q^{*1.3} \rightarrow \ell^* \simeq \left(\frac{2}{5}\right)^{k-1} L^*, \quad (6)$$

where L^* is the length of the first-order branches (i.e. $k = 1$). We note that the choice of different geometric laws for widths and lengths does not change the qualitative behavior of the model.

For modeling the response of the bifurcation we employ the previously introduced two-cell BRT model. The nodal relationship proposed by BRT for the transversal exchange of water (Q_y^*) and sediment (Qs_y^*) for a generic node of order k , taking into account (5), reads as follows:

$$\frac{Qs_{y_{z-1}}^*}{Q_{z-1}^*} = \frac{Q_{y_{z-1}}^*}{Q_{z-1}^*} - \mathcal{R} \left(\frac{4}{3}\right)^k \frac{\eta_{2z-1}^* - \eta_{2z}^*}{2D_0^*}, \quad z = 2^{k-1}, \dots, 2^k - 1, \quad (7)$$

with η^* the bed elevations of the two cells, αW_0^* long, which are able to exchange water and sediment upstream the bifurcation (for a detail of the two cells, see Fig. 4). Following RTB, the bed elevations in the two bifurcates are affected by the tidal motion, which induces a correction with respect to the normal flow of the order of $O(\epsilon^2)$. This correction turns out to be a function of the relative tidal amplitude at the downstream nodes (or the sea mouth in the case of the terminal branches), channels length, channels slope, and on the flow depth values in normal flow conditions. Taking advantage of the fact that ϵ is a small parameter, it can be proved that the water surface elevation and flow depth at each node have the following expressions [45] (see for details of the

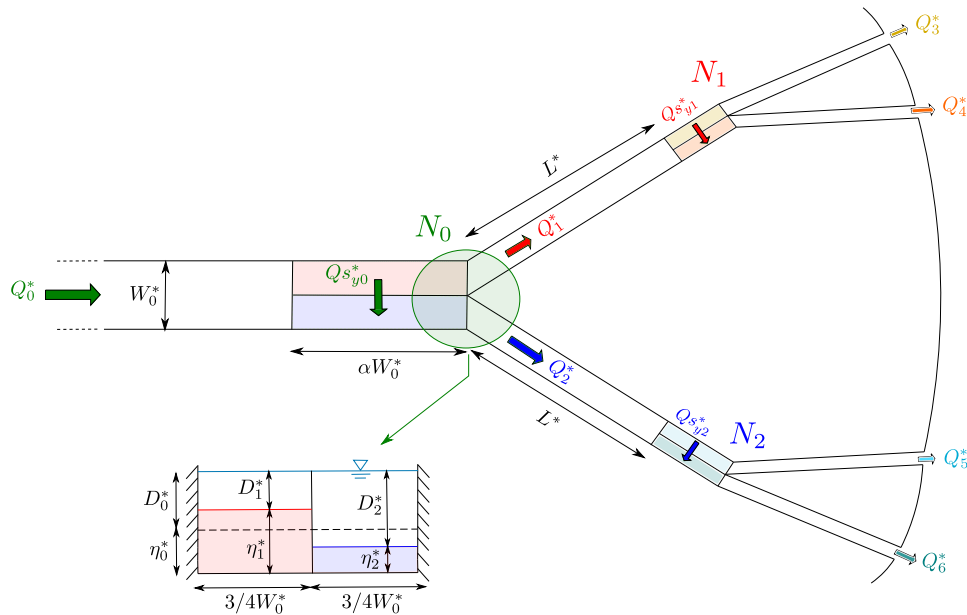


Figure 4: Plan view of the idealized micro-tidal network consisting of a total of seven branches coupled through three bifurcations. The geometry of the network is symmetric at each node, with channel lengths and widths assigned following the empirically-derived relations (5) and (6).

derivation [66, 22]):

$$H^* = L \frac{S}{S_0} D_0^* + \epsilon^2 D_u^{-1} \Theta(\Lambda) \left\{ \exp \left[-2\Re(\mu) L \frac{S}{S_0} D_u^{-1} \right] - 1 \right\} D_0^*, \quad (8a)$$

$$D^* = D_u D_0^* + \epsilon^2 D_u^{-1} \Psi(\Lambda) \exp \left[-2\Re(\mu) L \frac{S}{S_0} D_u^{-1} \right] D_0^*, \quad (8b)$$

with $\Lambda = \Lambda_0 D_u^{1/3} (S/S_0)^{-3/2}$, where the suffix $_u$ denotes the value of a quantity in normal flow conditions, and the expression for the coefficients Ψ , Θ , and μ are given in the Appendix.

In order to determine flow and bed topography in each channels, five internal (i.e. matching) conditions at the bifurcations node are required: the conservation of water and sediment mass, the equality of the water surface elevation for each cell, and the BRT relationship (7). At the end, for each node the following algebraic nonlinear system of equations is obtained:

$$Q_{z-1} = Q_{2z-1} + Q_{2z}, \quad (9a)$$

$$Q_{s_{z-1}} = Q_{s_{2z-1}} + Q_{s_{2z}}, \quad (9b)$$

$$H_{2z-1}|_{N_{z-1}} = H_{2z}|_{N_{z-1}}, \quad (9c)$$

$$\frac{Q_{s_{yz-1}}}{Q_{s_{z-1}}} = \frac{Q_{yz-1}}{Q_{z-1}} - \mathcal{R} \left(\frac{4}{3} \right)^k \frac{1}{\sqrt{4 S_{z-1}/S_0 D_{uz-1}}} (D_{2z} - D_{2z-1}), \quad (9d)$$

where the variables are made non-dimensional in the form:

$$D^* = D_0^* D, \quad L^* = L_{B0}^* L, \quad Q^* = Q_0^* Q, \quad Q_{s^*} = Q_{s_0^*} Q. \quad (10)$$

It is worth noting that tidal amplitude in the internal nodes depends on the amount of water and sediment delivered by the channels, and it can be computed through the following expression (see in the Appendix for the details about the derivation):

$$\epsilon|_{N_{z-1}} = \epsilon|_{N_{2z-1}} \exp \left[-\mu_{2z-1} \left(\frac{2}{5} \right)^{k-1} L D_{u_{2z-1}}^{-1} \frac{S_{2z-1}}{S_0} \right], \quad k \geq 2, \quad (11)$$

where $\epsilon|_{N_{z-1}}$ coincides with ϵ for the terminal branches. As expected, $\epsilon|_{N_{z-1}}$ tends to vanish over distances that are longer compared to the backwater length of the single branches.

Finally, we underline that the present analysis focuses on the long-term asymptotic equilibrium (i.e. steady) state of the system. Suppose each branch of the network in equilibrium (sec. [45]); this is equivalent to assume a much slower timescale of the bifurcates with respect to the timescale of the bifurcation, which in turn is slower than the tidal period. This hierarchy of timescales allows for studying the response of the network as a sequence of quasi-equilibrium states, where the effect of tidal fluctuations exhibits just by changing the (dimensionless) tidal amplitude ϵ .

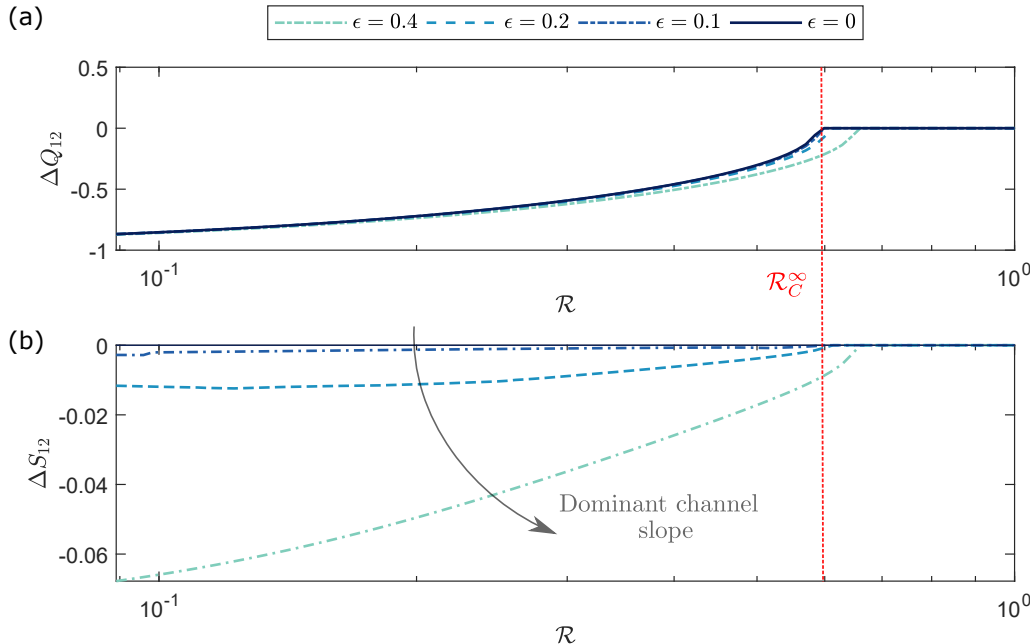


Figure 5: Equilibrium solution for the upstream node (N_0 , see Fig. 4) as a function of the bifurcation parameter \mathcal{R} , for increasing values of the tidal amplitude ϵ : (a) discharge asymmetry ΔQ_{12} ; (b) slope asymmetry ΔS_{12} . The critical threshold at which the unbalanced solution ($\Delta Q \neq 0$) appears decreases for higher values of ϵ , revealing the destabilizing effect of the tidal action on the apex bifurcation ($\Delta S < 0$). We note that just half-plot of the diagram is shown, as the solution is symmetric with respect to the \mathcal{R} -axis. The parameter \mathcal{R}_C^∞ denotes the critical threshold in the absence of tide. Parameters are: $\Lambda_0 = 10$, and $L = 0.3$.

4 CONTRASTING RESPONSE OF A DELTA NETWORK TO TIDAL ACTION

In analogy with the work of [16] and from observations showing that tide-influenced deltas are often composed by few number of distributaries [21, 51], we consider a simple network made up by two orders of bifurcations (i.e. $k = 2 \rightarrow N = 3$, see Eq. (4)). Thus, at the end the problem requires the solution of a nonlinear system of twelve algebraic equations, which can be cast in terms of the channel slopes and (dimensionless) normal flow depths of each channel, once suitable closure formulas for the sediment transport and friction are employed.

Sediment fluxes are computed by means of the Engelund & Hansen [67] formula:

$$Q_s = 0.05 C_f^{-1} \tau_*^{5/2} = Q_{s0} D_u^{17/6} \left(\frac{S}{S_0} \right)^{5/2}, \quad \tau_* = \frac{U_*^2 C_f}{\Delta g^* d^*} = \tau_{*0} D_u S / S_0, \quad (12)$$

where Δ is the relative submerged sediment density, and C_f is the friction coefficient, expressed through the Manning-Strickler formula:

$$C_f = \left(\frac{D_u^{*1/6}}{n^* \sqrt{g^*}} \right)^{-2}, \quad (13)$$

with n^* the Manning coefficient. Thanks to (13), the dimensionless water discharge is proportional to $Q \propto D_u^{5/3} \sqrt{S/S_0}$.

The model requires as input just few parameters, namely (Λ_0, \mathcal{R}) for the reference flow in the upstream channel, the scaled tidal amplitude at sea (ϵ), and the dimensionless length (L) of the first-order branches (i.e. 1, 2). To analyze the results, we rely on the following two asymmetry indexes [8], ΔS and ΔQ , which can be taken as representative metrics of each bifurcation node response:

$$\Delta Q = \frac{Q_{2z-1} - Q_{2z}}{Q_{z-1}}, \quad \Delta S = \frac{S_{2z-1} - S_{2z}}{S_0}, \quad z = 1, 2, 3. \quad (14)$$

From hereinafter, as the solution in the form of a pitchfork bifurcation shows a reflection symmetry with respect to the x-axis, we report just half-plot, namely the case when the branch 2 is dominant (i.e. $Q_1 < Q_2$). We emphasize that in the present problem there are no forcing effects potentially leading to a break-out of the symmetry. In other words, any externally-imposed slope advantage that may alter downstream rating curves is not considered.

In Fig. 5, the equilibrium solution relatively to the upstream node (i.e. N_0) is shown as a function of the bifurcation parameter \mathcal{R} and for increasing values of the tidal amplitude ϵ . When ϵ is gradually increased, the critical value of the bifurcation parameter

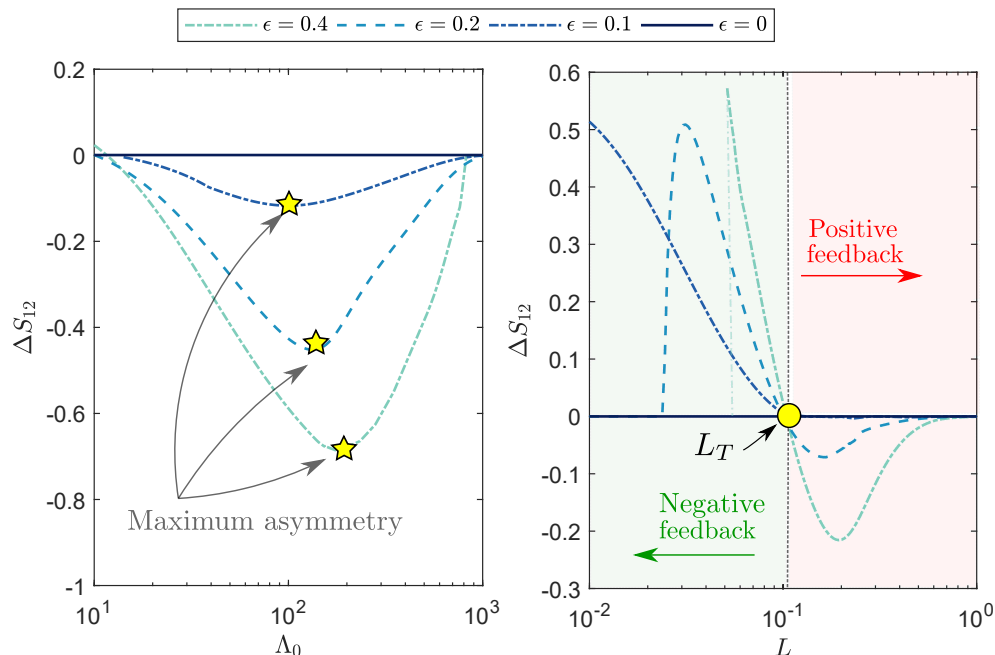


Figure 6: Slope asymmetry index in the upstream node (ΔS_{12}) relatively to parameters (a) Λ_0 ($L = 0.1$) and (b) dimensionless length of the branches L ($\Lambda_0 = 10$), for different values of the tidal amplitude ϵ . The threshold length L_T distinguishes the region of the plot where tide exerts a positive ($L > L_T$) or a negative ($L < L_T$) feedback. Both panels are obtained for a fixed $\mathcal{R} = 0.1$.

(\mathcal{R}_C) at which the balanced solution (i.e. $\Delta Q = 0$) becomes unstable gets larger (Fig. 5a). This behavior is associated with a positive feedback exerted by the tidal action on the apex bifurcation, which decreases the stability of the system (Fig. 5b). In other words, the model would suggest that when the bifurcation parameter \mathcal{R} is lower than the critical value \mathcal{R}_C , a greater fraction of water and sediment fluxes is steered towards one of the two downstream branches as tidal amplitude increases, promoting the development of an unbalanced configuration. In this case, water level variations at the internal nodes increase the slope of the dominant branch, thereby contributing to destabilize even further the system.

This notwithstanding, as introduced in Section 2.2 it is reasonable to suppose that \mathcal{R} takes on a minor role in fine-grained sand-bed rivers, where most of sediment is carried in suspension and therefore is weakly deflected by the gravitational pull at the bifurcation [68, 8]. In the limiting case $\mathcal{R} \rightarrow 0$, the sediment flux divides proportionally to the water discharge (see Eq. 7), and the stability of the bifurcation is fundamentally dominated by tide-induced effects. Specifically, for $\epsilon \neq 0$ the parameters Λ_0 and L control how tidal action affects flow and sediment distribution through variations of the energy slope tracked by the asymmetry index ΔS (Fig. 6). Differently from the discharge partition ΔQ , ΔS is highly sensible to a small variation of Λ_0 and L . As long as the tidal impact at apex node increases (i.e. higher values of Λ_0 and/or shorter branches) the degree of slope asymmetry augments up to a maximum (in absolute terms) due to a gradient advantage for the branch receiving more water and sediment: if $Q_1 < Q_2$, then $\epsilon_1 < \epsilon_2$ (see Eq. 11); consequently, channel 2 is steeper than channel 1 ($S_2 > S_1$) revealing that tidal action has a destabilizing effect. However, the scenario radically changes when the channels are shorter than a threshold length, L_T . When $L < L_T$ the sign of ΔS_{12} becomes positive. In these conditions $\epsilon_1 > \epsilon_2$, and thus the stability of the system is increased due to a steepening of the penalized branch, which in turn reduces the flux asymmetries between the bifurcates.

Let us now analyze what happens in the terminal branches (i.e. 3 to 6). In this case, the effect of tides is always stabilizing as found in the single bifurcation case by RTB (Fig. 7). The value of the threshold at which the bifurcations evolve toward an unbalanced equilibrium state increases, suggesting the tendency of the system to attain a more stable and balanced configuration for higher tidal amplitudes and values of Λ_0 with respect to the sole bifurcation. Differently from the apex node, the channel slope is higher in the penalized branch. In accordance with previous studies [42, 56, 44, 22], an increasing tidal influence results in a more even discharge partitioning in the terminal branches (i.e. reduced values of the discharge asymmetry ΔQ). Also in this case, the slope asymmetry shows a maximum. In other words, there is a value of Λ_0 , and thus of the ratio between the backwater length and flow magnitude (see Eq. 2), for which the stabilizing effect to tidal action is maximized.

Finally, we have noted that an additional order of bifurcations does not change the qualitative response of the system and the key drivers governing its stability.

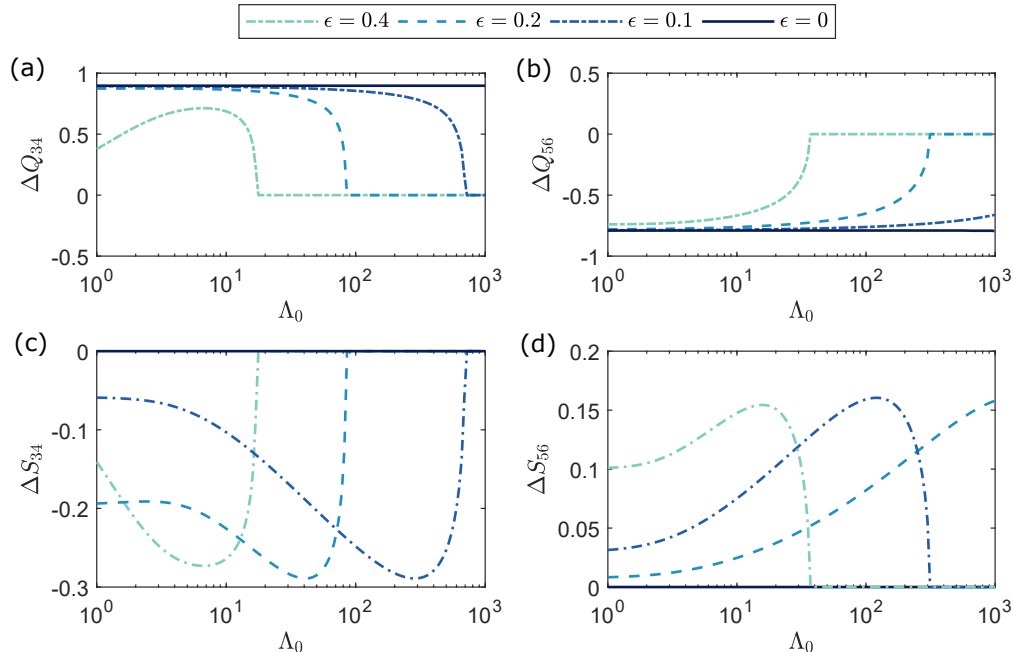


Figure 7: Equilibrium diagram for the downstream nodes (a,c) N_1 and (b,d) N_2 as a function of the parameter (Λ_0) and for increasing values of ϵ . Differently from the apex node, downstream bifurcations are always stabilized by tidal action: for stronger tides, the region of parameters that guarantees a symmetric discharge partitioning, enlarges. Parameters are: $\mathcal{R} = 0.1$ and $L = 1$.

5 DISCUSSION

The present results show that a contrasting response of bifurcations to tidal action arise even in a simple steady model of a delta network. As displayed in Fig. 8, the model suggests that there is a threshold of the reference parameters (i.e. $\mathcal{R}, \Lambda_0, \epsilon, L$) that separates two drastically different behaviors of the apex node. Specifically, let us consider this condition in terms of the channel lengths, with a fixed value of the other parameters and requiring that $\epsilon \neq 0$. In first instance, if L is lower than a critical value L_C water and sediment are equally distributed among the channels (Fig. 8a). The symmetric configuration becomes unstable for $L > L_C$ so that one of the two upstream branches is favored. The development of an unbalanced configuration is physically sustained through variations of the channel slopes, which in turn modify flow rating curves and sediment transport capacity of the two bifurcates. The slope asymmetry crucially depends from the length of the branches: if L is longer than a threshold L_T , tide promotes the allocation of a larger fraction of the incoming discharge towards the dominant channel since it is subject to a greater tidal amplitude, thus becoming steeper than the other channel (Fig. 8b). On the other hand, a stabilizing effect is observed for $L < L_T$ (Fig. 8c, lower-right panel). In this case the feedback reverses in sign: the bed slope of the branches carrying lower discharge can increase up to nearly two times the slope of the upstream reach, due to a negative feedback that tends to establish an even flow and sediment distribution. Conversely, the terminal branches are always stabilized by tidal action despite that they are clearly affected by flux diversion in the upstream node.

The pluralistic behavior described above also distinguishes, at least qualitatively, field [21, 51, 56], experimental [47] and numerical [70, 69] studies showing that tide-influenced deltas are often characterized by an initially-formed main (or few) active stem from which smaller distributary channels branch out, where tide acts to distribute uniformly flow and sediment across the network. The scouring action performed by tidal currents prevents bed aggradation, the main responsible for the formation/reoccupation of new/old channels through avulsion events in river-dominated deltas without tidal forcing, which are often dissected by a widespread number of branches radiating from the apex bifurcation [71].

In order to better address the significance of the picture portrayed so far, let us focus on some examples. In a series of recent laboratory experiments, Lentsch et al. [47] analyzed the effects of tides and sea-level rise on deltaic morphology. In pure riverine conditions (i.e. $\epsilon = 0$), a widespread number of channels are observed to dissect the subaerial surface of the delta, where frequent avulsion events are triggered by channels aggradation; the shifting of the maximum sediment flux among branches leads over time to a nearly symmetric planform shape of the delta. Differently, as tide is progressively increased, the number and lateral mobility of channels drop; in this case, a main thread distributes flow and sediment among few smaller branches originating towards the coastline, as schematized in the upper-right plot of Fig. 8c. Despite a straightforward comparison with the present model is not feasible, some instructive indications can be deduced: first, $\mathcal{R} < \mathcal{R}_C$ (computed from the RTB model), and thus in the absence of tides, any bifurcation should evolve asymmetrically; second, in spite of moderate tidal amplitudes ($0.4 \leq \epsilon \leq 1$), values of $\Lambda_0 \approx 2$,

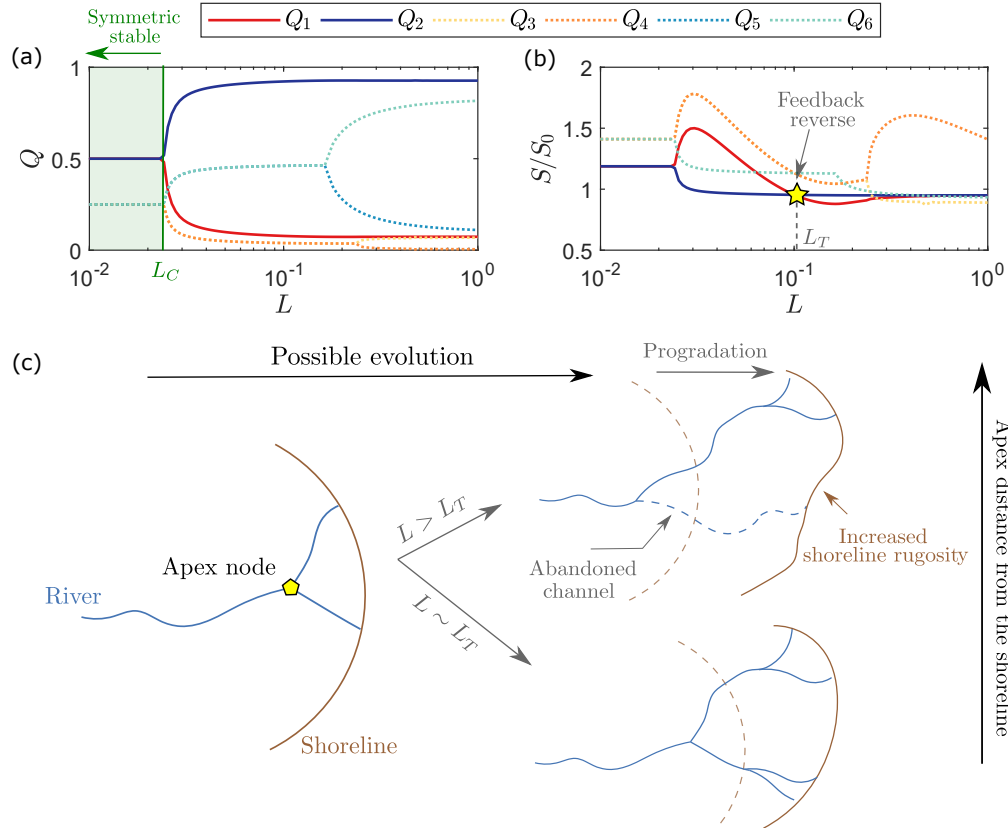


Figure 8: Equilibrium diagram for (a) flow discharge and (b) channel slope for each branch of the network, as a function of the average length L . Parameters are: $\epsilon = 0.2$, $\Lambda_0 = 10$, and $\mathcal{R} = 0.1$. (c) Conceptual model of the possible evolution towards the equilibrium of a tide-influenced delta: when $L > L_C > L_T$, tide promotes the development of an unbalanced configuration, possibly leading to the closure of one of the two branches. Under these condition the shoreline is expected to display a wrinkled pattern, as tide reduces the lateral mobility of the channels preventing avulsion events able to distribute sediment over the whole delta topset [69, 47]. Differently, if $L > L_C < L_T$ tide has a global stabilizing effect, which tends to reduce the inequalities in discharge partitioning among the branches. Consequently, the planform morphology of the delta is expected to develop a more symmetric shape.

$L_A \approx 1$ (see Fig. 3) suggest that tidal influence is rather modest; in this condition, $L > L_T$ and the development of an unbalanced configuration at the apex node is possibly sustained by tidal action.

Turning to a natural field example, the Mahakam Delta is often referred as a typical tide-influenced delta. Tide distinctly shows its fingerprint on the delta morphology, with funnel-shaped estuarine channels in the seaward reaches, often disconnected from the main distributaries [55]. In this case, compared to a value of the bifurcation parameter \mathcal{R} extremely small (i.e. $\mathcal{R} \approx 0.03$), the model reveals that tide is sufficiently strong to actively affect the upstream node ($\epsilon \approx 0.2$, $\Lambda_0 \approx 85$, $L_A \approx 0.1$), reducing the inequalities in discharge partitioning, as also indicated by previous numerical simulations [42]. Computed values of the critical parameters from the RTB model give an avulsion length L_A that is nearly equal to the critical threshold L_C discriminating between a stable/unstable balanced configuration (i.e. $L < L_T$).

A final case is the Wax Lake Delta, which represents a benchmark for the study of human-based solutions aimed at counteracting the sinking of many deltaic coastlines due to climate change, subsidence, and sediment starvation [72, 73, 74, 75]. The Wax Lake is an actively net-depositional delta subject to weak tides ($\epsilon \sim 10^{-2}$), with a progradation phase sustained by sediment deposition at the channels mouth [63]. It was observed [64] that just a small fraction of the total distributaries carry the higher fraction of the total sediment load. In this context, recent studies highlight the overlooked role of tidal flow-field modulation, which manifests primarily on the sediment exchange with interior islands and with erosion of the subaqueous delta front [76, 59], but it has also been suggested to balance discharge distribution [77]. The highly sensitivity of the Wax Lake to water level variations is expected by the extremely low value of $L_A \approx 0.03$, but despite of that, the model would indicate that a significant tidal impact on the equilibrium configuration of the deltaic bifurcations is not appreciable.

It is important to stress that the potential effect of short-term temporal changes as daily fluctuations in the water levels, different tidal propagation in the branches [77, 78], or due to wind-driven currents [11], are not accounted for by the model, which focuses

on the long-term morphodynamic equilibrium state. From a modeling perspective, relaxing the steady assumption leads to some interesting developments, which are inspired from field and numerical evidences of the deltas discussed so far. During a sequence of spring-neap cycles, the discharge division in a couple of bifurcations in the Mahakam Delta was observed to oscillate around an asymmetric state [42, 79]. Differently, in the Wax Lake Delta during this natural variation of the tidal cycle that occurs approximately every two weeks, the discharge partitioning over two branches oscillates around a nearly symmetric state (see Fig. 4 of [77]). Relaxing the steady assumption would allow to analyze the response of the system to time-varying (periodic) forcing, in a similar fashion to the work of Bertoldi et al. [27]. Bertoldi and co-workers studied experimentally and theoretically the effect of periodic downstream-migrating alternate bars interacting with a single fluvial bifurcation, which leads to an enriched and variegated dynamics. In a complementary way, throughout the paper we have recalled how flow oscillations are generated even without time-dependent external forcing, but rather due to differential deposition in the branches [14, 17]. A natural extension of the present model should include sediment deposition, incorporating into the single bifurcation model of Salter et al. [14], the tide-averaged effect following the framework of RTB.

Finally, along the paper we have avoided to discuss what happens in tide-dominated conditions (i.e. $\epsilon \gg O(1)$), representative of deltas like the Ganges-Brahmaputra-Meghna Delta, the Indus Delta, the Niger Delta [80, 81, 82], or in the coastal fringe of the Mahakam Delta [56]. Such networks diverge from the tree-like structure sketched in Fig. 4. The tidal plain is often characterized by tidal channels growing landward from the shoreline that frequently merge into secondary distributaries carrying freshwater and sediment, in turn generating looping patterns [83]. In these cases, the framework discussed herein must be abandoned in favor of a scheme explicitly including the interplay between riverine and bi-directional tidal flow. We note that a bifurcation model in purely tide-dominated conditions (i.e. in the absence of a fluvial supply of freshwater and sediment) is still lacking.

6 CONCLUSIONS

In this work, we have explored the long-term equilibrium configuration of a tide-influenced delta through a one-dimensional theoretical modeling. In order to understand the basic mechanisms underlying the response of the system, we have limited our analysis to a simple network composed by two orders of bifurcations. However, the model is general and the geometric configuration (i.e. widths, lengths, number of nodes) can be freely chosen, with the only restriction on the magnitude of tidal forcing, which has to satisfy the condition $\epsilon \ll 1$.

The following key outcomes are drawn:

- Differently from the single bifurcation case, tides can be either a stabilizing or a destabilizing factor for the asymptotic equilibrium state reached by the system. The model reveals that this contrasting response crucially depends from the relative tidal amplitude in the internal nodes, which is a function of the flow and sediment delivered from the apex bifurcation, and the ratio between the length of the channels and the backwater length.
- In the upstream node, there is a range of values of the reference parameters such that an initially stable symmetric bifurcation tends to become increasingly biased as the amplitude of tidal oscillations is increased. This behavior is associated to an increased tidal strength in the branch receiving more discharge, which tends to steepen with respect to the other branch. Nonetheless, if the tidal influence is sufficiently strong (e.g., the apex is progressively moved closer to the sea) the response of the system is reversed, and tide hinders the abandonment of one of the two anabranches by increasing the slope of the penalized branch, i.e. providing a stabilizing effect.
- Tides always exert a negative feedback in the terminal branches, reducing the inequalities in discharge partitioning that would occur in a pure riverine case.
- In accordance with previous works [10, 16], the model shows that tide-influenced delta networks behave as complex systems [12], where the overall response cannot be inferred without taking into account the coupling between upstream and downstream bifurcations.

ANALYTICAL EXPRESSION OF THE COEFFICIENTS μ , Ψ , AND Θ

In this section we provide the complete expressions for the coefficients appearing in Eqs. (8a-b). These coefficients are a function of the basic flow through the parameter Λ_0 , and of the specific channel characteristics through the dependence on D_u and S :

$$\mu = \frac{5}{3} \left[1 + \sqrt{1 + \frac{18}{25} i \Lambda} \right], \quad (15a)$$

$$\Psi = \frac{13}{8} + \frac{5}{2} \frac{\Lambda}{|\mu|^2} \left(\Im(\mu) + \frac{4}{11} \Lambda \right), \quad (15b)$$

$$\Theta = \frac{1}{2\Re(\mu)} \left[\frac{65}{36} + \frac{\Lambda}{|\mu|^2} \left(5\Im(\mu) + \frac{167}{66} \Lambda \right) \right], \quad (15c)$$

where i is the imaginary unit, and the functional dependence of $\Lambda = f(\Lambda_0, D_u, S/S_0)$ is given in the main text. We note that (15a-c) contribute to the magnitude of the tidal second-order correction (i.e. $\propto \epsilon^2$) that deviate flow variables (i.e. D, η, U) from the uniform conditions.

TIDAL AMPLITUDE IN THE INTERNAL NODES

The starting point for the derivation of Eq. (11) is the one-dimensional differential problem for the evolution of a single river-dominated estuary. Namely, the governing equations for each branch of the network are the continuity and momentum conservation for the fluid phase, coupled with the sediment mass balance:

$$\Lambda \frac{\partial D_u}{\partial t} + \frac{\partial q}{\partial \tilde{x}} = 0, \quad (16a)$$

$$\Lambda F_0^2 \frac{\partial}{\partial t} \left(\frac{q}{D_u} \right) + \frac{F_0^2}{2} \frac{\partial}{\partial \tilde{x}} \left(\frac{q^2}{D_u^2} \right) + \frac{\partial H}{\partial \tilde{x}} + \frac{q|q|}{D_u^{10/3}} = 0, \quad (16b)$$

$$\Lambda \mathcal{T} \frac{\partial}{\partial t} (H - D_u) + \frac{1}{(1-p)} \frac{\partial q_s}{\partial \tilde{x}} = 0, \quad (16c)$$

where p is the sediment porosity, $\tilde{x} = x D_u^{-1} S/S_0$ is a longitudinal coordinate with the origin at the sea (or from an internal node) and pointing landward, and $\mathcal{T} = q_0^* / \sqrt{\Delta g^* d^{*3}}$ is the ratio between the hydrodynamic timescale and ‘‘morphodynamic’’ timescale.

In the assumptions of micro-tidal conditions (i.e. $\epsilon \ll 1$) and $F_0^2 \sim \mathcal{F} \epsilon$, with \mathcal{F} an order $O(1)$ quantity, Seminara et al. [45] tackled system (16a-c) to find an analytical solution for the tidally-averaged morphodynamic equilibrium by means of a perturbation approach. Specifically, each variable of the problem is expanded in powers of ϵ as follows:

$$(q, D_u, H) = (q_0, D_{u0}, H_0) + \epsilon(q_1, D_{u1}, H_1) + \epsilon^2(q_2, D_{u2}, H_2) + O(\epsilon^3), \quad (17)$$

where we note that now the suffixes denote the subsequent perturbation orders.

Substituting from (17) into the governing system (16a-c), equating likewise powers of ϵ , a cascade of differential problems is then found. Here, with the aim of finding the super-elevation of the free surface with respect of the reference level (i.e. a flat free surface with $H_0 \propto L S/S_0$) moving landward along a channel from the shoreline, we are just interested in the order $O(\epsilon)$ part of the solution, which describes the propagation of a small amplitude wave. For the interested readers, we refer to [45] for the details of the analysis. The solution is expressed as:

$$(q_1, D_{u1}, H_1) = (0, D_{u10}(\tilde{x}), H_{10}(\tilde{x})) + (q_{11}, D_{u11}, H_{11})(e^{it} + \text{c.c.}), \quad (18)$$

where $t = t^* \omega^*$, and c.c. stands for the complex conjugate of a complex number. Note that the tidally-averaged discharge per unit width q does not differ from the leading-order value q_0 , thus q_{10} (i.e. the steady component) is zero.

Solving for the time-dependent part of the solution leads to the following differential problem in q_{11} :

$$\frac{d^2 q_{11}}{d\tilde{x}^2} + \frac{10}{3} \frac{dq_{11}}{d\tilde{x}} - 2i\Lambda q_{11} = 0, \quad (19a)$$

$$q_{11} = 0, \quad (\tilde{x} \rightarrow \infty), \quad (19b)$$

$$\frac{dq_{11}}{d\tilde{x}} = -\frac{i\Lambda}{2}, \quad (\tilde{x} = 0), \quad (19c)$$

where the multiplicative factor $1/2$ in the second boundary condition derives from the assumption of monochromatic tidal wave (i.e. $\propto \sin(t)$). The solution of (19a-c) gives the following expression for q_{11} :

$$q_{11} = \frac{i\Lambda}{2\mu} e^{-\mu\tilde{x}}. \quad (20)$$

In the assumption $H_{11} = D_{11}$ (during a single tidal cycle bed variations are negligible), from the sediment mass conservation, and substituting (20), it is obtained:

$$H_{11} = \frac{1}{2} e^{-\mu\tilde{x}}, \quad (21)$$

and Eq. (11) is readily found.

CONFLICT OF INTEREST

The authors declare that they have no conflict of interest.

REFERENCES

- [1] J. R. L. Allen. Morphodynamics of Holocene salt marshes: A review sketch from the Atlantic and Southern North Sea coasts of Europe. *Quaternary Science Reviews*, 19(12):1155–1231, 2000. ISSN 02773791. doi: 10.1016/S0277-3791(99)00034-7.
- [2] Rudy L. Slingerland and Norman D. Smith. River Avulsions and Their Deposits. *Annual Review of Earth and Planetary Sciences*, 32(1):257–285, 2004. ISSN 0084-6597. doi: 10.1146/annurev.earth.32.101802.120201.
- [3] Peter E. Ashmore. Morphology and Dynamics of Braided Rivers. In J. Shroder and Ellen Wohl, editors, *Treatise on Geomorphology*, volume 9, chapter 17, pages 289–312. Academic Press, San Diego, CA, 2013. ISBN 9780080885223. doi: 10.1016/B978-0-12-374739-6.00242-6.
- [4] Maarten G. Kleinhans, Robert I. Ferguson, Stuart N. Lane, and Richard J. Hardy. Splitting rivers at their seams: bifurcations and avulsion. *Earth Surface Processes and Landforms*, 38(1):47–61, 2013. ISSN 01979337. doi: 10.1002/esp.3268.
- [5] Hannah R. Dietterich and Katharine V. Cashman. Channel networks within lava flows: Formation, evolution, and implications for flow behavior. *Journal of Geophysical Research: Earth Surface*, 119:1704–1724, 2014. doi: 10.1002/2014JF003103.
- [6] Ajay B. Limaye, Jean Louis Grimaud, Steven Y.J. Lai, Brady Z. Foreman, Yuhei Komatsu, and Chris Paola. Geometry and dynamics of braided channels and bars under experimental density currents. *Sedimentology*, 65(6):1947–1972, 2018. ISSN 13653091. doi: 10.1111/sed.12453.
- [7] Michele Bolla Pittaluga, Giovanni Coco, and Maarten G. Kleinhans. A unified framework for stability of channel bifurcations in gravel and sand fluvial systems. *Geophysical Research Letters*, 42(18):7521–7536, 2015. ISSN 00948276. doi: 10.1002/2015GL065175.
- [8] Marco Redolfi, Guido Zolezzi, and Marco Tubino. Free and forced morphodynamics of river bifurcations. *Earth Surface Processes and Landforms*, 44(4):973–987, 2019. ISSN 10969837. doi: 10.1002/esp.4561.
- [9] Alejandro Tejedor, A. Longjas, I. Zaliapin, and Efi Foufoula-Georgiou. Delta channel networks: 1. A graph-theoretic approach for studying connectivity and steady state transport on deltaic surfaces. *Water Resources Research*, 51(6):3998–4018, 2015. ISSN 1093-474X. doi: 10.1002/2014WR016577.
- [10] Paola Passalacqua. The Delta Connectome: A network-based framework for studying connectivity in river deltas. *Geomorphology*, 277:50–62, 2017. ISSN 0169555X. doi: 10.1016/j.geomorph.2016.04.001.
- [11] Alice Sendrowski and Paola Passalacqua. Process connectivity in a naturally prograding river delta. *Water Resources Research*, 53:1841–1863, 2017. ISSN 1093-474X. doi: 10.1002/2016WR019768.
- [12] Mark. E. J. Newman. The Structure and Function of Complex Networks. *SIAM Review*, 45(2):167–256, 2003. ISSN 00361445. doi: 10.1137/S003614450342480.
- [13] Steven H. Strogatz. Exploring complex networks. *Nature*, 410(March):268–276, 2001.
- [14] Gerard Salter, Chris Paola, and Vaughan R. Voller. Control of Delta Avulsion by Downstream Sediment Sinks. *Journal of Geophysical Research: Earth Surface*, 123(1):142–166, 2018. ISSN 21699003. doi: 10.1002/2017JF004350.
- [15] Gerard Salter, Vaughan R. Voller, and Chris Paola. How does the downstream boundary affect avulsion dynamics in a laboratory bifurcation? *Earth Surface Dynamics*, 7:911–927, 2019. doi: 10.5194/esurf-2019-26.
- [16] Gerard Salter, Vaughan R. Voller, and Chris Paola. Chaos in a simple model of a delta network. *Proceedings of the National Academy of Sciences of the United States of America*, pages 1–18, 2020. doi: 10.1073/pnas.2010416117.
- [17] Douglas A. Edmonds, Austin J. Chadwick, Michael P. Lamb, Jorge Lorenzo-Trueba, Brad A. Murray, William Nardin, Gerard Salter, and John B. Shaw. Morphodynamic Modeling of River-Dominated Deltas : A Review and Future Perspectives. In *Treatise on Geomorphology*, pages 1–31. Elsevier Inc., 2 edition, 2021. ISBN 9780128182345. doi: 10.1016/B978-0-12-818234-5.00076-6.
- [18] Niccolò Ragno, Marco Redolfi, and Marco Tubino. Coupled Morphodynamics of River Bifurcations and Confluences. *Water Resources Research*, 57(1):1–26, 2021. ISSN 0043-1397. doi: 10.1029/2020WR028515.
- [19] Jaap H. Nienhuis, Andrew D. Ashton, and Liviu Giosan. What makes a delta wave-dominated? *Geology*, 43(6):511–514, 2015. ISSN 19432682. doi: 10.1130/G36518.1.
- [20] Douglas J. Jerolmack and John B. Swenson. Scaling relationships and evolution of distributary networks on wave-influenced deltas. *Geophysical Research Letters*, 34(23):1–5, 2007. ISSN 00948276. doi: 10.1029/2007GL031823.
- [21] Cornel Olariu and Janok P. Bhattacharya. Terminal distributary channels and delta front architecture of river-dominated delta systems. *Journal of Sedimentary Research*, 76:212–233, 2006. doi: 10.2110/jsr.2006.026.
- [22] Niccolò Ragno, Nicoletta Tambroni, and Michele Bolla Pittaluga. Effect of Small Tidal Fluctuations on the Stability and Equilibrium Configurations of Bifurcations. *Journal of Geophysical Research: Earth Surface*, 125(8):1–20, 2020. doi: 10.1029/2020JF005584.
- [23] Zheng Bing Wang, M. De Vries, R. J. Fokkink, and A. Langerak. Stability of river bifurcations in 1D morphodynamic models. *Journal of Hydraulic Research*, 33(6):739–750, 1995. ISSN 00221686. doi: 10.1080/00221689509498549.

- [24] Rudy L. Slingerland and Norman D. Smith. Necessary conditions for a meandering-river avulsion. *Geology*, 26(5):435–438, 1998. ISSN 00917613. doi: 10.1130/0091-7613(1998)026<0435:NCFAMR>2.3.CO;2.
- [25] Marco Redolfi, Guido Zolezzi, and Marco Tubino. Free instability of channel bifurcations and morphodynamic influence. *Journal of Fluid Mechanics*, 799:476–504, 2016. ISSN 14697645. doi: 10.1017/jfm.2016.389.
- [26] Walter Bertoldi and Marco Tubino. River Bifurcations: Experimental observations on equilibrium configurations. *Water Resources Research*, 43(10), 2007. doi: 10.1029/2007WR005907.
- [27] Walter Bertoldi, Luca Zanon, Stefano Miori, Rodolfo Repetto, and Marco Tubino. Interaction between migrating bars and bifurcations in gravel bed rivers. *Water Resources Research*, 45(6), 2009. ISSN 00431397. doi: 10.1029/2008WR007086.
- [28] Robert E. Thomas, Daniel R. Parsons, Steven D. Sandbach, Gareth M. Keevil, Wouter A. Marra, Richard J. Hardy, James L. Best, Stuart N. Lane, and Jessica A. Ross. An experimental study of discharge partitioning and flow structure at symmetrical bifurcations. *Earth Surface Processes and Landforms*, 36(15):2069–2082, 2011. ISSN 01979337. doi: 10.1002/esp.2231.
- [29] Douglas A. Edmonds and Rudy L. Slingerland. Stability of delta distributary networks and their bifurcations. *Water Resources Research*, 44(9):1–13, 2008. ISSN 00431397. doi: 10.1029/2008WR006992.
- [30] Maarten G. Kleinhans, H. R.A. Jagers, Erik Mosselman, and C. J. Sloff. Bifurcation dynamics and avulsion duration in meandering rivers by one-dimensional and three-dimensional models. *Water Resources Research*, 44(8):1–31, 2008. ISSN 00431397. doi: 10.1029/2007WR005912.
- [31] Annunziato Siviglia, Guglielmo Stecca, Davide Vanzo, Guido Zolezzi, Eleuterio F. Toro, and Marco Tubino. Numerical modelling of two-dimensional morphodynamics with applications to river bars and bifurcations. *Advances in Water Resources*, 52:243–260, 2013. ISSN 03091708. doi: 10.1016/j.advwatres.2012.11.010.
- [32] T. B. Le, Alessandra Crosato, Erik Mosselman, and Wim S.J. Uijttewaai. On the stability of river bifurcations created by longitudinal training walls. Numerical investigation. *Advances in Water Resources*, 113(July 2017):112–125, 2018. ISSN 03091708. doi: 10.1016/j.advwatres.2018.01.012.
- [33] M. Paul Mosley. Response of Braided Rivers to Changing Discharge. *Journal of Hydrology (NZ)*, 22(1):18–67, 1983.
- [34] Leif M. Burge. Stability, morphology and surface grain size patterns of channel bifurcation in gravel-cobble bedded anabranching rivers. *Earth Surface Processes and Landforms*, 31(10):1211–1226, 2006. ISSN 01979337. doi: 10.1002/esp.1325.
- [35] Guido Zolezzi, Walter Bertoldi, and Marco Tubino. Morphological analysis and prediction of river bifurcations. In G H Best, J L Bristow, and C S Petts, editors, *Braided Rivers: Process, Deposits, Ecology and Management*, volume 36, pages 233–256. Blackwell, 2006. ISBN 9781405151214. doi: 10.1002/9781444304374.ch11.
- [36] Walter Bertoldi. Life of a bifurcation in a gravel-bed braided river. *Earth Surface Processes and Landforms*, 37(12):1327–1336, 2012. ISSN 01979337. doi: 10.1002/esp.3279.
- [37] Michele Bolla Pittaluga, Rodolfo Repetto, and Marco Tubino. Channel bifurcation in braided rivers: Equilibrium configurations and stability. *Water Resources Research*, 39(3):1–13, 2003. ISSN 0043-1397. doi: 10.1029/2001WR001112.
- [38] K. W. Olesen. Alternate bars in and meandering of alluvial river. Technical report, Delft University of Technology, 1983.
- [39] Gary Parker. Lateral Bed Load Transport on Side Slopes. *Journal of Hydraulic Engineering*, 110(2):197–199, 1984.
- [40] Stephen Wiggins. *Introduction to Applied Nonlinear Dynamical Systems and Chaos*. Springer, 2003. ISBN 0387001778. doi: 10.2307/3620310.
- [41] F. A. Buschman, A. J. F. Ton Hoitink, Maarten van der Vegt, and P. Hoekstra. Subtidal flow division at a shallow tidal junction. *Water Resources Research*, 46(12):1–12, 2010. ISSN 00431397. doi: 10.1029/2010WR009266.
- [42] Maximiliano G. Sassi, A. J.F. Hoitink, Benjamin De Brye, Bart Vermeulen, and Eric Deleersnijder. Tidal impact on the division of river discharge over distributary channels in the Mahakam Delta. *Ocean Dynamics*, 61(12):2211–2228, 2011. ISSN 16167341. doi: 10.1007/s10236-011-0473-9.
- [43] A. J.F. Hoitink and D. A. Jay. Tidal river dynamics: Implications for deltas. *Reviews of Geophysics*, 54(1):240–272, 2016. ISSN 19449208. doi: 10.1002/2015RG000507.
- [44] Arya P. Iwamoto, Maarten Van Der Vegt, and Maarten G. Kleinhans. Morphological evolution of bifurcations in tide-influenced deltas. *Earth Surface Dynamics*, 8(2):413–429, 2020. ISSN 2196632X. doi: 10.5194/esurf-8-413-2020.
- [45] Giovanni Seminara, Michele Bolla Pittaluga, and Nicoletta Tambroni. Morphodynamic equilibrium of tidal channels. In W. Rodi and M. Uhlmann, editors, *Environmental Fluid Mechanics: Memorial Volume in Honour of Prof. Gerhard H. Jirka*, chapter 8, pages 153–174. CRC Press, 2012. ISBN 9780203803967. doi: 10.1201/b12283.
- [46] Chris Paola and David Mohrig. Palaeohydraulics revisited: palaeoslope estimation in coarse-grained braided rivers. *Basin Research*, 8:243–254, 1996. doi: 10.1046/j.1365-2117.1996.00253.x.
- [47] Nathan Lentsch, Alvis Finotello, and Chris Paola. Reduction of deltaic channel mobility by tidal action under rising relative sea level. *Geology*, 46(7):599–602, 2018. ISSN 19432682. doi: 10.1130/G45087.1.

- [48] W. E. Galloway. Process framework for describing the morphologic and stratigraphic evolution of deltaic depositional systems. In M. L. Broussard, editor, *Deltas, Models for Exploration*, pages 87–98. Houston Geol. Surv., Houston, Tx, 1975.
- [49] Jaap H. Nienhuis, Andrew D. Ashton, Douglas A. Edmonds, A.J.F.Ton Hoitink, A. J. Kettner, Joel C. Rowland, and Torbjörn E. Törnqvist. Global-scale human impact on delta morphology has led to net land area gain. *Nature*, 577(7791): 514–518, 2020. ISSN 14764687. doi: 10.1038/s41586-019-1905-9.
- [50] H. J. Walker. Arctic Deltas. *Journal of Coastal Research*, 14(3):718–738, 1998. doi: 10.2307/4298831.
- [51] James P.M. Syvitski and Yoshiki Saito. Morphodynamics of deltas under the influence of humans. *Global and Planetary Change*, 57(3–4):261–282, 2007. ISSN 09218181. doi: 10.1016/j.gloplacha.2006.12.001.
- [52] Jaap H. Nienhuis, A. J.F.Ton Hoitink, and Torbjörn E. Törnqvist. Future Change to Tide-Influenced Deltas. *Geophysical Research Letters*, 45(8):3499–3507, 2018. ISSN 19448007. doi: 10.1029/2018GL077638.
- [53] Sam A.S. Brooke, Vamsi Ganti, Austin J. Chadwick, and Michael P. Lamb. Flood Variability Determines the Location of Lobe-Scale Avulsions on Deltas: Madagascar. *Geophysical Research Letters*, 47(20):1–12, 2020. ISSN 19448007. doi: 10.1029/2020GL088797.
- [54] Anastasia Piliouras and Joel C. Rowland. Arctic River Delta Morphologic Variability and Implications for Riverine Fluxes to the Coast. *Journal of Geophysical Research: Earth Surface*, 125(1):1–20, 2020. ISSN 21699011. doi: 10.1029/2019JF005250.
- [55] Maximiliano G. Sassi, A. J. F. Ton Hoitink, Benjamin De Brye, and Eric Deleersnijder. Downstream hydraulic geometry of a tidally influenced river delta. *Journal of Geophysical Research: Earth Surface*, 117(4):1–13, 2012. ISSN 01480227. doi: 10.1029/2012JF002448.
- [56] A. J. F. Ton Hoitink, Zheng Bing Wang, Bart Vermeulen, Y. Huismans, and Karl Kästner. Tidal controls on river delta morphology. *Nature Geoscience*, 10(9):637–645, 2017. ISSN 17520908. doi: 10.1038/ngeo3000.
- [57] Austin J. Chadwick, Michael P. Lamb, A. J. Moodie, Gary Parker, and Jeffrey A. Nittrouer. Origin of a Preferential Avulsion Node on Lowland River Deltas. *Geophysical Research Letters*, 46(8):4267–4277, 2019. ISSN 19448007. doi: 10.1029/2019GL082491.
- [58] Douglas A. Edmonds, Rudy L. Slingerland, Jim Best, Daniel R. Parsons, and Norman D. Smith. Response of river-dominated delta channel networks to permanent changes in river discharge. *Geophysical Research Letters*, 37(12):1–5, 2010. ISSN 00948276. doi: 10.1029/2010GL043269.
- [59] Matthew Hiatt and Paola Passalacqua. Hydrological connectivity in river deltas: The first-order importance of channel-island exchange. *Water Resources Research*, 51:2264–2282, 2015. doi: 10.1002/2014WR016149.
- [60] Alejandro Tejedor, Anthony Longjas, Douglas A. Edmonds, Ilya Zaliapin, Tryphon T. Georgiou, Andrea Rinaldo, and Efi Foufoula-Georgiou. Entropy and optimality in river deltas. *Proceedings of the National Academy of Sciences of the United States of America*, 114(44):11651–11656, 2017. ISSN 10916490. doi: 10.1073/pnas.1708404114.
- [61] Tian Y. Dong, Jeffrey A. Nittrouer, Brandon McElroy, Elena Il'icheva, Maksim Pavlov, Hongbo Ma, Andrew J. Moodie, and Vsevolod M. Moreido. Predicting Water and Sediment Partitioning in a Delta Channel Network Under Varying Discharge Conditions. *Water Resources Research*, 56(11):1–21, 2020. ISSN 19447973. doi: 10.1029/2020WR027199.
- [62] Hans André. *Development of the Laitaure Delta, Swedish Lapland: A Study of Growth, Distributary Forms and Processes*. Number 88. Uppsala University, Uppsala, Sweden, Uppsala, 1994. ISBN 9150610686.
- [63] Douglas A. Edmonds and Rudy L. Slingerland. Mechanics of river mouth bar formation: Implications for the morphodynamics of delta distributary networks. *Journal of Geophysical Research: Earth Surface*, 112(2):1–14, 2007. ISSN 21699011. doi: 10.1029/2006JF000574.
- [64] Douglas A. Edmonds, Chris Paola, David C.J.D. Hoyal, and Ben A. Sheets. Quantitative metrics that describe river deltas and their channel networks. *Journal of Geophysical Research: Earth Surface*, 116(4):1–15, 2011. ISSN 21699011. doi: 10.1029/2010JF001955.
- [65] Hansjörg Seybold, José S. Andrade, and Hans J. Herrmann. Modeling river delta formation. *Proceedings of the National Academy of Sciences of the United States of America*, 104(43):16804–16809, 2007.
- [66] Michele Bolla Pittaluga, Nicoletta Tambroni, Alberto Canestrelli, Rudy L. Slingerland, Stefano Lanzoni, and Giovanni Seminara. Where river and tide meet: The morphodynamic equilibrium of alluvial estuaries. *Journal of Geophysical Research: Earth Surface*, pages 75–94, 2015. doi: 10.1002/2014JF003233.
- [67] Frank Engelund and Eggert Hansen. A monograph on sediment transport in alluvial streams. *Technical University of Denmark Ostervoldgade 10, Copenhagen K.*, 1967.
- [68] Karl Kästner and A.J.F.Ton Hoitink. Flow and Suspended Sediment Division at Two Highly Asymmetric Bifurcations in a River Delta : Implications for Channel Stability. *Journal of Geophysical Research: Earth Surface*, 124:1–23, 2019. doi: 10.1029/2018JF004994.

- [69] Valentina Marzia Rossi, Wonsuck Kim, Julio Leva López, Douglas A. Edmonds, Nathanael Geleynse, Cornel Olariu, Ronald J. Steel, Matthew Hiatt, and Paola Passalacqua. Impact of tidal currents on delta-channel deepening, stratigraphic architecture, and sediment bypass beyond the shoreline. *Geology*, 44(11):927–930, 2016. ISSN 19432682. doi: 10.1130/G38334.1.
- [70] Nathanaël Geleynse, Joep E.A. Storms, Dirk Jan R. Walstra, H. R. Albert Jagers, Zheng B. Wang, and Marcel J.F. Stive. Controls on river delta formation; insights from numerical modelling. *Earth and Planetary Science Letters*, 302(1-2): 217–226, 2011. ISSN 0012821X. doi: 10.1016/j.epsl.2010.12.013.
- [71] Meredith D. Reitz, Douglas J. Jerolmack, and John B. Swenson. Flooding and flow path selection on alluvial fans and deltas. *Geophysical Research Letters*, 37(6):1–5, 2010. ISSN 00948276. doi: 10.1029/2009GL041985.
- [72] Chris Paola, Robert R. Twilley, Douglas A. Edmonds, Wonsuck Kim, David Mohrig, Gary Parker, Enrica Viparelli, and Vaughan R. Voller. Natural Processes in Delta Restoration: Application to the Mississippi Delta. *Annual Review of Marine Science*, 3(1):67–91, 2011. ISSN 1941-1405. doi: 10.1146/annurev-marine-120709-142856.
- [73] Austin J. Chadwick, Michael P. Lamb, and Vamsi Ganti. Accelerated river avulsion frequency on lowland deltas due to sea-level rise. *Proceedings of the National Academy of Sciences of the United States of America*, 117(30):17584–17590, 2020. ISSN 10916490. doi: 10.1073/pnas.1912351117.
- [74] A. J. F. Hoitink, Jeffrey A. Nittrouer, Paola Passalacqua, John B. Shaw, E. J. Langendoen, Y. Huismans, and D. S. van Maren. Resilience of River Deltas in the Anthropocene. *Journal of Geophysical Research: Earth Surface*, 125(3):1–24, 2020. ISSN 21699011. doi: 10.1029/2019JF005201.
- [75] Brandee N. Carlson, Jeffrey A. Nittrouer, Travis E. Swanson, Andrew J. Moodie, Tian Y. Dong, Hongbo Ma, Gail C. Kineke, Minglong Pan, and Yuanjiang Wang. Impacts of engineered diversions and natural avulsions on delta-lobe stability. *Geophysical Research Letters*, 48:1–11, 2021. ISSN 0094-8276. doi: 10.1029/2021gl092438.
- [76] John B. Shaw and David Mohrig. The importance of erosion in distributary channel network growth , Wax Lake Delta , Louisiana. *Geological Society Of America*, pages 1–4, 2014. doi: 10.1130/G34751.1.
- [77] R. Wayne Wagner and David C. Mohrig. Flow and Sediment Flux Asymmetry in a Branching Channel Delta. *Water Resources Research*, 55:1–15, 2019. ISSN 19447973. doi: 10.1029/2019WR026050.
- [78] Jinyang Wang, Huib E. de Swart, and Yoeri M. Dijkstra. Dependence of tides and river water transport in an estuarine network on river discharge, tidal forcing, geometry and sea level rise. *Continental Shelf Research*, 225(June):104476, 2021. ISSN 18736955. doi: 10.1016/j.csr.2021.104476.
- [79] Maximiliano G. Sassi, A. J.F.Ton Hoitink, Bart Vermeulen, and H. Hidayat. Sediment discharge division at two tidally influenced river bifurcations. *Water Resources Research*, 49(4):2119–2134, 2013. ISSN 00431397. doi: 10.1002/wrcr.20216.
- [80] Robert W. Dalrymple and Kyungsik Choi. Morphologic and facies trends through the fluvial-marine transition in tide-dominated depositional systems: A schematic framework for environmental and sequence-stratigraphic interpretation. *Earth-Science Reviews*, 81(3-4):135–174, 2007. ISSN 00128252. doi: 10.1016/j.earscirev.2006.10.002.
- [81] Paola Passalacqua, Stefano Lanzoni, Chris Paola, and Andrea Rinaldo. Geomorphic signatures of deltaic processes and vegetation: The Ganges-Brahmaputra-Jamuna case study. *Journal of Geophysical Research: Earth Surface*, 118(3): 1838–1849, 2013. ISSN 21699011. doi: 10.1002/jgrf.20128.
- [82] R. L. Bain, R. P. Hale, and S. L. Goodbred. Flow Reorganization in an Anthropogenically Modified Tidal Channel Network: An Example From the Southwestern Ganges-Brahmaputra-Meghna Delta. *Journal of Geophysical Research: Earth Surface*, 124(8):2141–2159, 2019. ISSN 21699011. doi: 10.1029/2018JF004996.
- [83] Adam Konkol, Jon Schwenk, Eleni Katifori, and John Burnham Shaw. Interplay of river and tidal forcings promotes loops in coastal channel networks. *arXiv*, pages 1–7, 2021. doi: arXiv:2108.04151.